Hindawi
Security and Communication Networks
Volume 2024, Article ID 9757195, 1 page
https://doi.org/10.1155/2024/9757195

Retraction

Retracted: Noise-Tolerant Zeroing Neural Dynamics for Solving Hybrid Multilayered Time-Varying Linear Equation System

Security and Communication Networks

Received 8 January 2024; Accepted 8 January 2024; Published 9 January 2024

This article has been retracted by Hindawi following an investigation undertaken by the publisher [1]. This investigation has uncovered evidence of one or more of the following indicators of systematic manipulation of the publication process:

(1) Discrepancies in scope
(2) Discrepancies in the description of the research reported
(3) Discrepancies between the availability of data and the research described
(4) Inappropriate citations
(5) Incoherent, meaningless and/or irrelevant content included in the article
(6) Manipulated or compromised peer review

The presence of these indicators undermines our confidence in the integrity of the article's content and we cannot, therefore, vouch for its reliability. Please note that this notice is intended solely to alert readers that the content of this article is unreliable. We have not investigated whether authors were aware of or involved in the systematic manipulation of the publication process.

Wiley and Hindawi regrets that the usual quality checks did not identify these issues before publication and have since put additional measures in place to safeguard research integrity.

We wish to credit our own Research Integrity and Research Publishing teams and anonymous and named external researchers and research integrity experts for contributing to this investigation.

The corresponding author, as the representative of all authors, has been given the opportunity to register their agreement or disagreement to this retraction. We have kept a record of any response received.

References

[1] J. Li, Y. Shi, Y. Sun, J. Fan, and M. A. Mirza, "Noise-Tolerant Zeroing Neural Dynamics for Solving Hybrid Multilayered Time-Varying Linear Equation System," *Security and Communication Networks*, vol. 2022, Article ID 6040463, 13 pages, 2022.

Hindawi
Security and Communication Networks
Volume 2022, Article ID 6040463, 13 pages
https://doi.org/10.1155/2022/6040463

Research Article

Noise-Tolerant Zeroing Neural Dynamics for Solving Hybrid Multilayered Time-Varying Linear Equation System

Jian Li [1] Yang Shi [2] Yange Sun [1] Jianwei Fan [1] and Mohammed Aquil Mirza [3]

[1] *School of Computer and Information Technology, Xinyang Normal University, Xinyang 464000, China*
[2] *School of Information Engineering, Yangzhou University, Yangzhou 225127, China*
[3] *Department of Building and Real Estate, The Hong Kong Polytechnic University (PolyU), Hongkong, China*

Correspondence should be addressed to Jian Li; lijcit@xynu.edu.cn

Received 23 January 2022; Accepted 14 March 2022; Published 29 May 2022

Academic Editor: Xingsi Xue

Resource allocation problem in a wireless sensor network can be formulated as time-varying optimization, which can be further converted as time-varying linear equation system (TVLES). Hybrid multilayered time-varying linear equation system (HMTVLES) involving hybrid multilayers and time-variation characteristic is a complicated and challenging problem. Recently it has been solved by zeroing neural dynamics (ZND) method under ideal conditions, i.e., without noises. However, noises are ubiquitous, immanent and unavoidable in real-time systems. In this work, we propose a noise-tolerant zeroing neural dynamics (NTZND) model for solving HMTVLES. It can deal with different kinds of noises such as constant noise, linear-increasing noise, and random noise. Theoretical analyses guarantee the precision of NTZND model in the presence of different kinds of noises. In addition, a general NTZND model is proposed based on general activation function. Besides, classical ZND method and gradient neural dynamics (GND) method are also investigated and compared. Numerical experimental results are presented to verify the theoretical results of proposed models.

1. Introduction

Noises are ubiquitous, immanent and unavoidable in reality [1–10], such as resource allocation problem in a wireless sensor network [1, 2] and robot control [4–6]. Noises have different forms, such as constant noises, linear noises and random noises. For example, constant noises may exist if the hardware wear results in a fixed deviation. Random noises may exist due to sudden changes in the external environment. Noises existing in linear equation system solving process is necessary to be suppressed as many problems in reality are formulated as linear equation system, in which noises exist [9, 11]. There are many methods to solve classical linear equation system (i.e., time-invariant linear equation system) [12–16], such as decomposition, Gaussian elimination, and Jacobi iteration.

The rapid development of industry makes real-time computation increasingly required in industrial engineering. More and more researchers have investigated time-varying systems [17–23], which can better describe real-time feature than time-invariant ones. In [1, 2], resource allocation problem in a wireless sensor network was formulated as time-varying optimization, which can be further converted as time-varying linear equation system (TVLES) [6]. Specifically, the resource allocation problem is formulated as time-varying convex optimization under time-varying linear equality constraints. Then, we use Lagrangian multiplier method, and then the optimization can be converted as TVLES after calculating the partial derivatives. TVLES, which originates from time-invariant linear equation system, has been investigated [24–28]. Zeroing neural dynamics (ZND) method is a good alternative for solving TVLES [11, 21, 27–35]. ZND is also called Zhang neural dynamics and Zhang neural network, which is a special class of recurrent neural network and originates from Hoefeld neural network [21, 27, 28]. In [24], a unified finite-time convergence ZND model was proposed for time-varying linear equations, and the ZND model is applied to robotic applications. In [25], a new ZND model with varying-parameter was proposed to solve time-varying overdetermined system of linear equations. In [27], TVLES with time-varying rank-deficient coefficient was investigated and solved by a new discrete-time ZND model with least-squares solution obtained. In addition, in [11], a noise-suppressing neural model was proposed for solving the time-varying system of linear equations in a control-based approach perspective.

Classical time-varying problems are single-layered, which have relatively weak ability to describe practical problems [36–40]. Recently, by introducing multilayers in time-varying problems, multilayered time-varying problems are investigated [41–45]. For example, in [37], multilayered time-varying linear systems including equality and inequality layers were investigated by ZND method. In [39], general discrete-time ZND model with 7-instant was proposed for solving multilayered time-varying system with nonlinear inequality layer and linear equation layer. In [45], multilayered time-varying nonlinear equation system was investigated and solved and the proposed model was further applied to robot manipulator control. In addition, in [36], multilayered time-varying linear equation system (MTVLES) was solved by ZND method.

For better describing practical problems, hybrid multilayered time-varying linear equation system (HMTVLES) was investigated in [46], which is generated by adding a hybrid structure into MTVLES. The problem of HMTVLES was investigated and solved by ZND method in [46]. However, most researches about multilayered time-varying problems including HMTVLES do not consider noises and the problem solving is in idea conditions. Inspired by [3–6], in this work, we propose a noise-tolerant zeroing neural dynamics (NTZND) model for solving HMTVLES. It can deal with different kinds of noises such as constant noise, linear-increasing noise and random noise. Theoretical analyses guarantee the precision of NTZND model in the presence of different kinds of noises. In addition, a general NTZND model is proposed based on general activation function. Besides, classical ZND method and gradient neural dynamics (GND) method [47, 48] are also investigated and compared. Numerical experimental results are presented to verify the theoretical results of proposed models. The main contributions of this work are listed as follows:

(1) NTZND model is proposed for solving HMTVLES in the presence of different kinds of noises such as constant noise, linear-increasing noise and random noise.
(2) The effectiveness and precision of NTZND model in the presence of different kinds of noises are analyzed and guaranteed by theoretical analyses.
(3) General NTZND model is proposed based on general activation function. The corresponding theoretical analyses are provided.

The remainder of this paper is organized into five sections. Section 2 shows preliminaries including problem formulation and classical ZND and GND methods are introduced, and then, NTZND model is proposed to solve the problem of HMTVLES. Section 3 provides some theorems to guarantee the effectiveness and precision of NTZND model in the presence of different kinds of noises. Section 4 proposes a general NTZND model to solve the problem of HMTVLES. Section 5 illustrates numerical experimental results to verify the theoretical results. Section 6 concludes this work with final remarks.

2. Preliminaries and Motivations

In this section, preliminaries including problem formulation and classical ZND and GND methods [18, 27] are introduced, and then, NTZND model is proposed to solve the problem of HMTVLES. For the convenience of readers, abbreviations in this paper are summarized in Table 1.

2.1. Problem Formulation and Definitions. The problem formulation of HMTVLES originates from MTVLES and TVLES. In this subsection, problem formulation and definitions are revisited and shown as follows.

Definition 1. The time-invariant linear equation system [13] is defined as

$$A\mathbf{x} = \mathbf{b}, \tag{1}$$

where $A \in \mathbb{R}^{m\times n}$ is a time-invariant full-rank matrix with $m \le n$; $\mathbf{b} \in \mathbb{R}^{m}$ is a time-invariant vector; and $\mathbf{x} \in \mathbb{R}^{n}$ is unknown and to be solved.

Adding time variable t into time-invariant linear equation system (1) leads to TVLES as follows.

Definition 2. The time-varying linear equation system (TVLES) [24] is defined as

$$A(t)\mathbf{x}(t) = \mathbf{b}(t), \tag{2}$$

where $A(t) \in \mathbb{R}^{m\times n}$ is a time-varying matrix with $m \le n$, which is assumed to be always full-rank over time; $\mathbf{b}(t) \in \mathbb{R}^{m}$ is a time-varying vector; and $\mathbf{x}(t) \in \mathbb{R}^{n}$ is unknown and to be solved.

By introducing two layers on the basis of TVLES (2), in which one layer is with respect to $\mathbf{x}(t)$ and the other is with respect to its time-derivative $\dot{\mathbf{x}}(t)$, the MTVLES is constructed as follows.

Definition 3. The multilayered time-varying linear equation system (MTVLES) [36] is defined as

$$\begin{aligned} A(t)\mathbf{x}(t) &= \mathbf{b}(t),\\ C(t)\dot{\mathbf{x}}(t) &= \mathbf{d}(t), \end{aligned} \tag{3}$$

where $A(t) \in \mathbb{R}^{m_1\times n}$ and $C(t) \in \mathbb{R}^{m_2\times n}$ are time-varying matrices with $m_1 + m_2 \le n$, which are assumed to be always full-rank over time; $\mathbf{b}(t) \in \mathbb{R}^{m}$ is a time-varying vector; and $\mathbf{x}(t) \in \mathbb{R}^{n}$ is unknown and to be solved, such that two layers of (3) are satisfied.

Table 1: Abbreviations and their explanations.

Abbreviation	Explanation
TVLES	Time-varying linear equation system
MTVLES	Multilayered time-varying linear equation system
HMTVLES	Hybrid multilayered time-varying linear equation system
ZND	Zeroing neural dynamics
GND	Gradient neural dynamics
NTZND	Noise-tolerant zeroing neural dynamics

Furthermore, designing a hybrid structure in the second layer of MTVLES (3), we have the HMTVLES as follows.

Definition 4. The hybrid multilayered time-varying linear equation system (HMTVLES) [46] is defined as

$$\begin{aligned} A(t)\mathbf{x}(t) &= \mathbf{b}(t), \\ C(t)\dot{\mathbf{x}}(t) + E(t)\mathbf{x}(t) &= \mathbf{d}(t), \end{aligned} \tag{4}$$

where $A(t) \in \mathbb{R}^{m_1 \times n}$, $C(t) \in \mathbb{R}^{m_2 \times n}$ and $E(t) \in \mathbb{R}^{m_2 \times n}$ are time-varying matrices with $m_1 + m_2 \leq n$, in which the combination of $A(t)$ and $C(t)$ is assumed to be always full-rank over time; $\mathbf{b}(t) \in \mathbb{R}^m$ is a time-varying vector; and $\mathbf{x}(t) \in \mathbb{R}^n$ is unknown and to be solved, such that two layers of (4) are satisfied.

2.2. ZND and GND Models for HMTVLES. ZND method is an alternative to solve HMTVLES [46]. The constructive process of ZND model is as follows.

First, on the basis of the first layer of HMTVLES (4), a vector-form error function is defined as

$$\varepsilon(t) := A(t)\mathbf{x}(t) - \mathbf{b}(t). \tag{5}$$

Second, dynamics formula is designed to make error function (5) tend to be zero vector, which means that the designed dynamics formula is applied to every elements of error function. We define any element of error function as $\varepsilon_i(t)$ with $i = 1, 2, \ldots, m_1$, and dynamics formula is designed as

$$\dot{\varepsilon}_i\ (t) = -\lambda\varphi(\varepsilon_i(t)), \tag{6}$$

where λ is a positive constant, which is utilized to adjust the convergent rate of the proposed models. $\varphi(\cdot)$ is the activation function, which must be a monotonically-increasing odd activation function [7]. The following monotonically increasing odd activation functions are frequently used to construct the ZND models.

(1) Linear activation function [7]:

$$\varphi(\varepsilon_i(t)) = \varepsilon_i(t). \tag{7}$$

(2) Power activation function [7]:

$$\varphi(\varepsilon_i(t)) = \varepsilon_i^p(t), \tag{8}$$

where $p \geq 3$ is an odd integer.

(3) Biexponential activation function [7]:

$$\varphi(\varepsilon_i(t)) = \exp(\kappa\varepsilon_i(t)) - \exp(-\kappa\varepsilon_i(t)), \tag{9}$$

where $\kappa = 3$.

(4) Power-sigmoid activation function [7]:

$$\varphi(\varepsilon_i(t)) = \begin{cases} \varepsilon_i^p(t), & \text{if } \left|\varepsilon_i(t)\right| \geq 1, \\ \dfrac{1+\exp(-q)}{1-\exp(-q)}\dfrac{1-\exp(-q\varepsilon_i(t))}{1+\exp(-q\varepsilon_i(t))}, & \text{else,} \end{cases} \tag{10}$$

where $p \geq 3$ and $q > 2$.

Third, substituting error function (5) into dynamics formula 6 yields the equivalency equation of the first-layer of HMTVLES (4) as follows:

$$A(t)\dot{\mathbf{x}}(t) = -\lambda\varphi(\varepsilon(t)) - \dot{A}(t)\mathbf{x}(t) + \dot{\mathbf{b}}(t). \tag{11}$$

Finally, combining the equivalency (11) and the second layer of HMTVLES (4) yields ZND model as follows:

$$\begin{bmatrix} A(t) \\ C(t) \end{bmatrix} \dot{\mathbf{x}}(t) = \begin{bmatrix} -\lambda\varphi(\varepsilon(t)9) - \dot{A}(t)\mathbf{x}(t) + \dot{\mathbf{b}}(t) \\ \mathbf{d}(t) - E(t)\mathbf{x}(t) \end{bmatrix}. \tag{12}$$

For the convenience of comparison, ZND model with measurement noises is shown as follows:

$$\begin{bmatrix} A(t) \\ C(t) \end{bmatrix} \dot{\mathbf{x}}(t) = \begin{bmatrix} -\lambda\varphi(\varepsilon(t)) - \dot{A}(t)\mathbf{x}(t) + \dot{\mathbf{b}}(t) + \eta(t) \\ \mathbf{d}(t) - E(t)\mathbf{x}(t) \end{bmatrix}, \tag{13}$$

where $\eta(t)$ is vector-form measurement noises, such as constant noises, time-varying linear noises, random noises.

GND method is an alternative to solve TVLES, while it fails to solve HMTVLES (4) [36, 46]. For the convenience of comparison, the constructive process of GND model to solve HMTVLES (4) is as follows.

First, we define an energy function as

$$\epsilon(t) = \|A(t)\mathbf{x}(t) - \mathbf{b}(t)\|_2^2. \tag{14}$$

Second, the GND design formula is employed to make the energy function (14) tend to be zero, which is shown as follows:

$$\dot{\mathbf{x}}(t) = -\lambda\frac{\partial\epsilon(t)}{\partial\mathbf{x}(t)}, \tag{15}$$

where the parameter $\lambda > 0$.

Third, substituting energy function (14) into GND design (15) yields the equivalency equation of the first-layer of HMTVLES (4) as follows:

$$\dot{\mathbf{x}}(t) = -\lambda A^T(t)(A(t)\mathbf{x}(t) - \mathbf{b}(t)), \tag{16}$$

where T is the transposition operator.

Finally, combining the equivalency (16) and the second layer of HMTVLES (4) yields GND model as follows:

$$\begin{bmatrix} I \\ C(t) \end{bmatrix} \dot{\mathbf{x}}(t) = \begin{bmatrix} -\lambda A^T(t)(A(t)\mathbf{x}(t) - \mathbf{b}(t)) \\ \mathbf{d}(t) - E(t)\mathbf{x}(t) \end{bmatrix}. \quad (17)$$

GND model with measurement noises is shown as follows:

$$\begin{bmatrix} I \\ C(t) \end{bmatrix} \dot{\mathbf{x}}(t) = \begin{bmatrix} -\lambda A^T(t)(A(t)\mathbf{x}(t) - \mathbf{b}(t)) + \eta(t) \\ \mathbf{d}(t) - E(t)\mathbf{x}(t) \end{bmatrix}. \quad (18)$$

Note that the matrix on the left side of $\dot{\mathbf{x}}(t)$ in GND model (17) belong $\mathbb{R}^{(n+m_2)\times n}$. GND model (17) could be viewed as overdetermined equation, and thus it may fail to solve HMTVLES (4).

2.3. NTZND Model for HMTVLES. Noises are ubiquitous, immanent and unavoidable in real-time systems. Traditional ZND and GND methods can not deal with noises well. In this subsection, we propose NTZND model for solving HMTVLES (4) with different measurement noises. Specifically, on the basis of error function (5), a novel dynamics formula is employed as follows [4, 7]:

$$\dot{\varepsilon}_i(t) = -\lambda \varepsilon_i(t) - \gamma \int_0^t \varepsilon_i(\tau) \mathrm{d}\tau. \quad (19)$$

Substituting error function (5) into dynamics (19) yields the equivalency equation of the first-layer of HMTVLES (4) as follows:

$$A(t)\dot{\mathbf{x}}(t) = -\lambda \varepsilon(t) - \gamma \int_0^t \varepsilon(\tau)\,\mathrm{d}\tau - \dot{A}(t)\mathbf{x}(t) + \dot{\mathbf{b}}(t). \quad (20)$$

Defining $\int_0^t \varepsilon(\tau)\mathrm{d}\tau$ as $\mathbf{y}(t)$, we have

$$\begin{aligned} &\begin{bmatrix} I & 0 \\ 0 & A(t) \end{bmatrix} \begin{bmatrix} \dot{\mathbf{y}}(t) \\ \dot{\mathbf{x}}(t) \end{bmatrix}, \\ &= \begin{bmatrix} A(t)\mathbf{x}(t) - \mathbf{b}(t) \\ -\lambda \varepsilon(t) - \gamma \mathbf{y}(t) - \dot{A}(t)\mathbf{x}(t) + \dot{\mathbf{b}}(t) \end{bmatrix}, \end{aligned} \quad (21)$$

where $I \in \mathbb{R}^{m_1 \times m_1}$ is identity matrix.

Combining (21) and the second layer of HMTVLES (4) yields NTZND model as follows:

$$F(t)\dot{\mathbf{z}}(t) = \mathbf{g}(t), \quad (22)$$

where

$$F(t) = \begin{bmatrix} I & 0 \\ 0 & A(t) \\ 0 & C(t) \end{bmatrix}, \quad \dot{\mathbf{z}}(t) = \begin{bmatrix} \dot{\mathbf{y}}(t) \\ \dot{\mathbf{x}}(t) \end{bmatrix}, \quad (23)$$

$$\mathbf{g}(t) = \begin{bmatrix} A(t)\mathbf{x}(t) - \mathbf{b}(t) \\ -\lambda \varepsilon(t) - \gamma \mathbf{y}(t) - \dot{A}(t)\mathbf{x}(t) + \dot{\mathbf{b}}(t) \\ \mathbf{d}(t) - E(t)\mathbf{x}(t) \end{bmatrix}. \quad (24)$$

NTZND model (22) with measurement noises is shown as follows:

$$F(t)\dot{\mathbf{z}}(t) = \mathbf{g}(t), \quad (25)$$

where

$$\mathbf{g}(t) = \begin{bmatrix} A(t)\mathbf{x}(t) - \mathbf{b}(t) \\ -\lambda \varepsilon(t) - \gamma \mathbf{y}(t) - \dot{A}(t)\mathbf{x}(t) + \dot{\mathbf{b}}(t) + \eta(t) \\ \mathbf{d}(t) - E(t)\mathbf{x}(t) \end{bmatrix}. \quad (26)$$

3. Theoretical Results and Analyses

Theorem 1. *Assume that $A(t) \in \mathbb{R}^{m_1 \times n}$, $C(t) \in \mathbb{R}^{m_2 \times n}$ and $E(t) \in \mathbb{R}^{m_2 \times n}$ are time-varying matrices with $m_1 + m_2 \le n$, in which the combination of $A(t)$ and $C(t)$ is assumed to be always full-rank over time, when the solution of NTZND model (22) starts from any initial state $\mathbf{x}(0)$, residual error defined as $\|A(t)\mathbf{x}(t) - \mathbf{b}(t)\|_2 + \|C(t)\dot{\mathbf{x}}(t) + E(t)\mathbf{x}(t) - \mathbf{d}(t)\|_2$ globally converges to zero as $t \longrightarrow +\infty$, where $\|\cdot\|_2$ denotes the 2-norm of vectors.*

Proof 1. See Appendix A for details. □

Theorem 2. *Residual error of NTZND model (22) for solving HMTVLES (4) exponentially converges to zero as $t \longrightarrow +\infty$.*

Proof 1. See Appendix B for details. □

Theorem 3. *Residual error of NTZND model (22) for solving HMTVLES (4) in the presence of unknown vector-form constant noise $\eta(t) = \eta \in \mathbb{R}^{m_1}$, i.e., model (23), converges to zero as $t \longrightarrow +\infty$.*

Proof 3. See Appendix C for details. □

Theorem 4. *Residual error of NTZND model (22) for solving HMTVLES (4) in the presence of unknown vector-form linear-increasing noise $\eta(t) = \eta t \in \mathbb{R}^{m_1}$, i.e., model (23), converges to η/γ as $t \longrightarrow +\infty$.*

Proof 4. See Appendix D for details. □

Theorem 5. *Residual error of NTZND model (22) for solving HMTVLES (4) in the presence of unknown vector-form random noise $\eta(t) \in \mathbb{R}^{m_1}$, i.e., model (23), is approximately in inverse proportion to λ as $t \longrightarrow +\infty$.*

Proof 5. See Appendix E for details. □

4. General NTZND Model

To develop NTZND model, the following dynamics formula is employed:

$$\dot{\varepsilon}_i(t) = -\lambda \varepsilon_i(t) - \gamma \int_0^t \varepsilon_i(\tau)\,\mathrm{d}\tau, \quad (27)$$

in which we simply use linear activation function. More other activation functions can be employed, such as power activation function, biexponential activation function, power-sigmoid activation function. Any monotonically increasing odd activation functions can be used. Thus, we define general monotonically increasing odd activation function as $\varphi(\cdot)$ [7]. The general dynamics formula is

$$\dot{\varepsilon}_i\ (t) = -\lambda\varphi\left(\varepsilon_i(t)\right) - \gamma\int_0^t \varepsilon_i(\tau)\,\mathrm{d}\tau, \tag{28}$$

Substituting error function (5) into general dynamics formula (24) yields the equivalency equation of the first-layer of HMTVLES (4) as follows:

$$A(t)\dot{\mathbf{x}}(t) = -\lambda\varphi(\varepsilon(t)) - \gamma\int_0^t \varepsilon(\tau)\,\mathrm{d}\tau - \dot{A}(t)\mathbf{x}(t) + \dot{\mathbf{b}}(t). \tag{29}$$

Finally, general NTZND model is obtained as follows:

$$F(t)\dot{\mathbf{z}}(t) = \mathbf{g}(t), \tag{30}$$

where

$$F(t) = \begin{bmatrix} I & 0 \\ 0 & A(t) \\ 0 & C(t) \end{bmatrix},\quad \dot{\mathbf{z}}(t) = \begin{bmatrix} \dot{\mathbf{y}}(t) \\ \dot{\mathbf{x}}(t) \end{bmatrix}, \tag{31}$$

$$\mathbf{g}(t) = \begin{bmatrix} A(t)\mathbf{x}(t) - \mathbf{b}(t) \\ -\lambda\varphi(\varepsilon(t)) - \gamma\mathbf{y}(t) - \dot{A}(t)\mathbf{x}(t) + \dot{\mathbf{b}}(t) \\ \mathbf{d}(t) - E(t)\mathbf{x}(t) \end{bmatrix}. \tag{32}$$

The convergence of general NTZND model (26) is proved in the following theorem.

Theorem 6. *Assume that $A(t) \in \mathbb{R}^{m_1\times n}$, $C(t) \in \mathbb{R}^{m_2\times n}$ and $E(t) \in \mathbb{R}^{m_2\times n}$ are time-varying matrices with $m_1 + m_2 \le n$, in which the combination of $A(t)$ and $C(t)$ is assumed to be always full-rank over time and that $\varphi(\cdot)$ is monotonically-increasing odd activation function, when the solution of general NTZND model (26) starts from any initial state $\mathbf{x}(t_0)$, residual error globally converges to zero as $t \longrightarrow +\infty$.*

Proof 6. See Appendix F for details. □

5. Numerical Results and Verifications

In this section, numerous numerical results are presented to verify the theoretical results shown as aforementioned. Codes can be found here at https://github.com/lijcit/1511895678. Specifically, we take HMTVLES (4) with $A(t) \in \mathbb{R}^{4\times 9}, \mathbf{b}(t) \in \mathbb{R}^4, \mathbf{x}(t) \in \mathbb{R}^9, C(t) \in \mathbb{R}^{4\times 9}, \mathbf{d}(t) \in \mathbb{R}^4$ as an example. By defining each elements of matrices and vectors as $A_{i,j}(t), b_{i,j}(t), C_i(t), E_{i,j}(t)$ and $d_i(t)$ $(i = 1, 2, 3, 4$ and $j = 1, \ldots, 9)$, their expressions are as follows:

$$A_{i,j}(t) = \begin{cases} \dfrac{\sin(0.1(i-j)t)}{j-i}, & \text{when } i > j, \\ \sin(0.1\mathrm{it}) + 3, & \text{when } i = j, \\ \dfrac{\cos 0.1((j-i)t)}{j-i}, & \text{when } i < j, \end{cases}$$

$$b_i 0(t) = \begin{cases} \cos(t), & \text{when } i \text{ is odd}, \\ \sin(0.5t), & \text{when } i \text{ is even}, \end{cases}$$

$$C_{i,j}(t) = \begin{cases} -\dfrac{\sin(0.1(i+4-j)t)}{i-j+4}, & \text{when } i+4 > j, \\ \sin(0.6t) + 3, & \text{when } i+4 = j, \\ \dfrac{\cos(0.1(j-i-4)t)}{j-i-4}, & \text{when } i+4 < j, \end{cases} \tag{33}$$

$$E_{i,j}(t) = \begin{cases} \dfrac{\sin(0.1(i-j)t)}{j-i}, & \text{when } i > j, \\ \sin(0.1\mathrm{it}) + 3, & \text{when } i = j, \\ \dfrac{\cos(0.1(j-i)t)}{j-i}, & \text{when } i < j, \end{cases}$$

$$\mathrm{d}_i(t) = \begin{cases} \cos(0.5t), & \text{when } i \text{ is odd}, \\ \sin(t), & \text{when } i \text{ is even}. \end{cases} \tag{34}$$

This HMTVLES satisfies the assumptions that $m_1 + m_2 \le n$ with $m_1 = m_2 = 4, n = 9$ and that combination of $A(t)$ and $C(t)$ is always full-rank over time.

First, to illustrate the effectiveness of NTZND model (22) without noise, a group of numerical experiments about NTZND model (22) with different values of parameters λ and γ are conducted. The corresponding numerical results are shown in Figure 1. It is observed that, by randomly setting initial state $\mathbf{x}(0)$, norm-form residual errors of NTZND model (22) with with different values of parameters all exponentially converge to zero. The results verify the theoretical results of Theorems 1 and 2. Besides, solution trajectories generated by NTZND model (22) are also presented.

Second, to illustrate the performances and superiority of NTZND model (22) in the presence of constant noise, i.e., model (23), different constant noises are added in to the solution process. For comparison, ZND model (13) and GND model (18) are also employed. Numerical results are

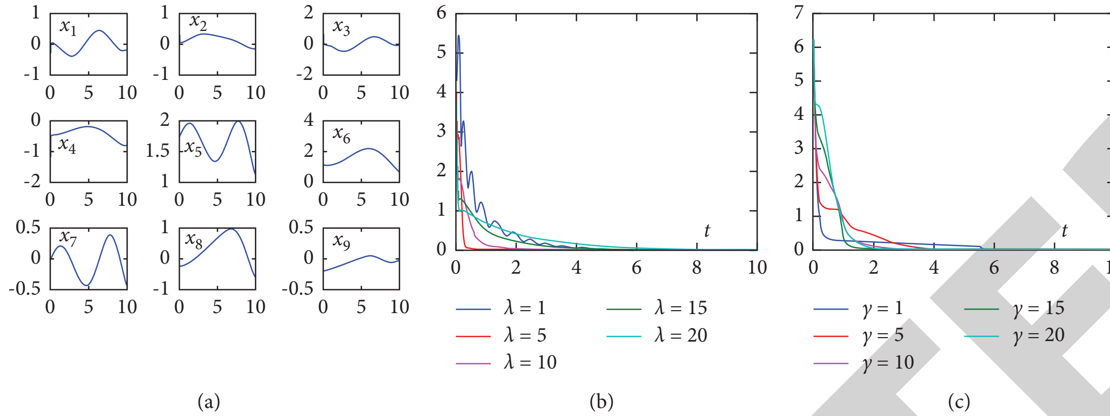

FIGURE 1: Solution trajectories and residual errors defined as $\|A(t)\mathbf{x}(t) - \mathbf{b}(t)\|_2 + \|C(t)\dot{\mathbf{x}}(t) + E(t)\mathbf{x}(t) - \mathbf{d}(t)\|_2$ when using NTZND model (22) to solve HMTVLES (4) with different values of λ and γ. (a) Solution trajectories. (b) Residual error with different values of λ. (c) Residual error with different values of γ.

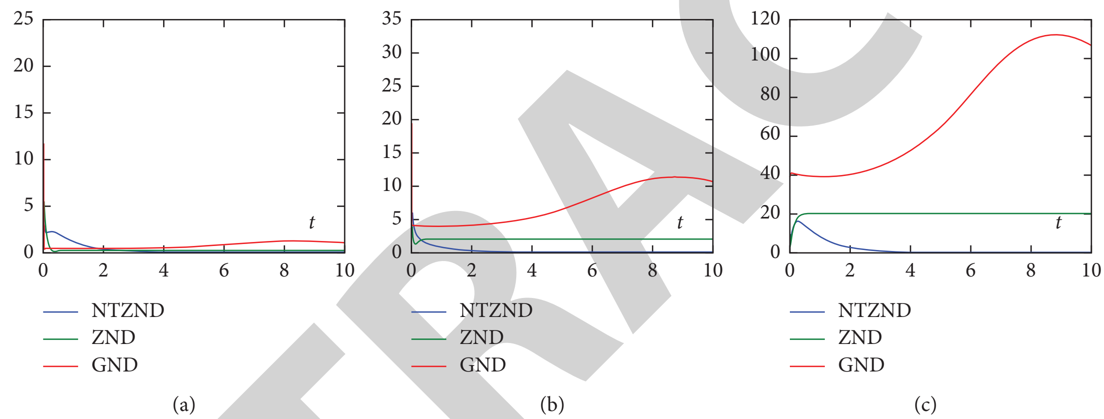

FIGURE 2: Residual errors when using NTZND model (23), ZND model (13) and GND model (18) to solve HMTVLES (4) in the presence of different constant noises. (a) With noise $\eta = 1$. (b) With noise $\eta = 10$. (c) With noise $\eta = 100$.

shown in Figure 2. It is observed that, when different values of constant noises are added, NTZND model (23) performs well and converges to zero. In contrast, ZND model (13) and GND model (18) fail to deal with constant noises and even diverge with large constant noise. The numerical results coincide with the results in Theorem 3.

Third, to illustrate the performances and superiority of NTZND model (22) in the presence of linear-increasing noise, i.e., model (23), linear-increasing noises are added into the solution process. Numerical results are shown in Figure 3. It is observed that, NTZND model (23) performs well while ZND model (13) and GND model (18) fail to deal with linear-increasing noises. In addition, to illustrate the relationship of solution precision and parameter γ, different values of γ are considered. From the numerical result, the solution precision is approximately inversely proportional to parameter γ, which coincides with the result in Theorem 4.

Fourth, to illustrate NTZND model (22) in the presence of random noise, i.e., model (23), random noises are added in to the solution process. Numerical results are shown in Figure 4. NTZND model (23) still performs well while GND model (18) fails to deal with linear-increasing noises. ZND model (13) can deal with random noise although the precision is lower than model (23). In addition, to illustrate the relationship of solution precision and parameter λ, different values of λ are considered. From the numerical result, the solution precision is approximately inversely proportional to parameter λ, which coincides with the result in Theorem 5.

Finally, to illustrate general NTZND model (26) in the presence of different kinds of noises, more numerical experiments about general NTZND model (26) with different

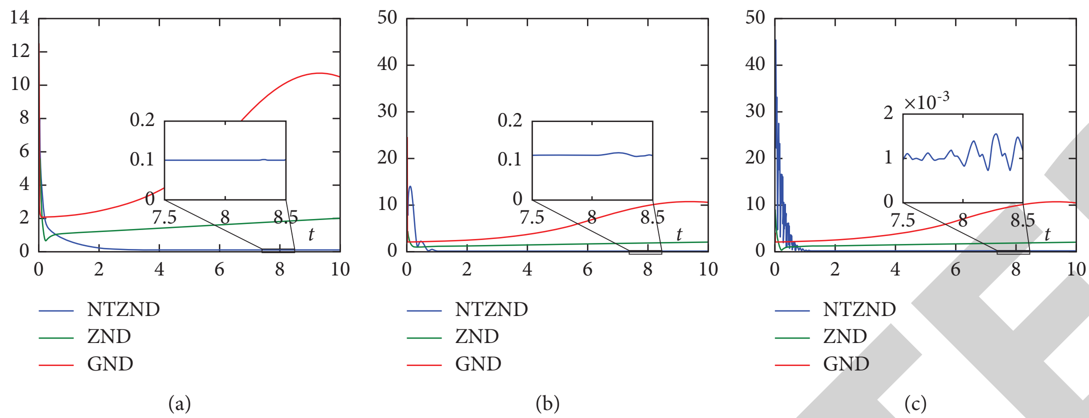

FIGURE 3: Residual errors when using NTZND model (23), ZND model (13) and GND model (18) to solve HMTVLES (4) in the presence of linear-increasing noise with different values of γ. (a) With $\gamma = 10$. (b) With $\gamma = 100$. (c) With $\gamma = 1000$.

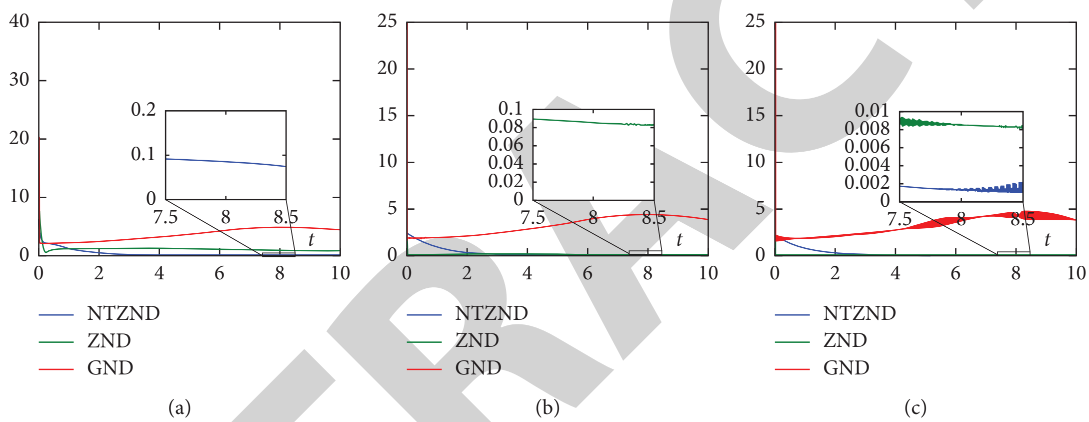

FIGURE 4: Residual errors when using NTZND model (23), ZND model (13) and GND model (18) to solve HMTVLES (4) in the presence of random noise with different values of λ. (a) With $\lambda = 10$. (b) With $\lambda = 100$. (c) With $\lambda = 1000$.

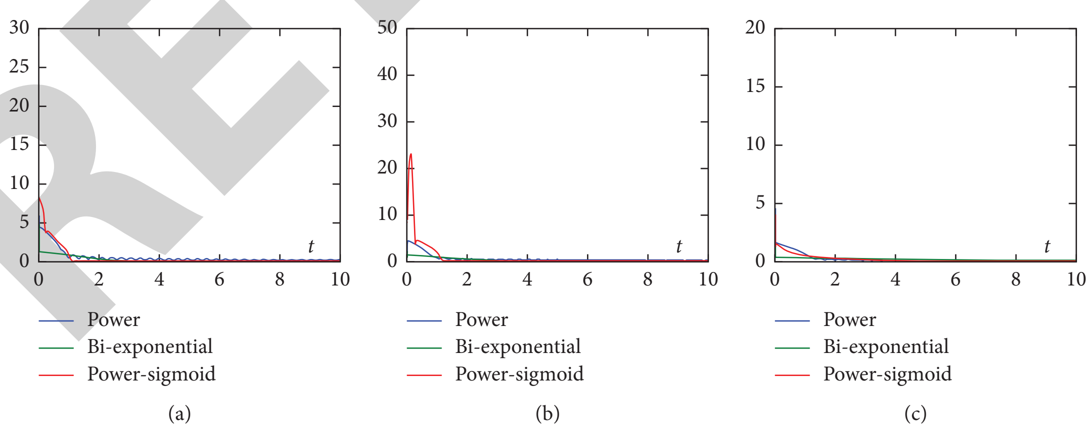

FIGURE 5: Residual errors when using general NTZND model (26) with different activation functions to solve HMTVLES (4) in the presence of different kinds of noises. (a) Constant noise. (b) Linear-increasing noise. (c) Random noise.

activation functions are conducted, and numerical results are shown in Figure 5. It is observed that a group of models generated by general NTZND model (26) with different activation functions exponentially converge in the presence of different kinds of noises, which coincides with the result in Theorem 6.

6. Conclusions

In this work, NTZND model (22) has been proposed to solve HMTVLES (4) in the presence of different kinds of noises (i.e., constant noises, linear-increasing noises and random noises). Classical ZND model (13) and GND model in the presence of different kinds of noises (18) have been introduced and investigated to substantiate the superiority of proposed NTZND model (22). Theoretical analyses have been provided to guarantee the effectiveness and precision of proposed model. Furthermore, general NTZND model (26) has been proposed based on general activation function.

Appendix

A. Proof Process of Theorem 1

As we assume that $m_1 + m_2 \leq n$, the number of constraints of linear equation system is not more than the number of variables, and thus the linear equation system is not over-determined. Besides, the combination of $A(t)$ and $C(t)$ is always full-rank, and thus HMTVLES (4) is solvable.

To verify the global convergence of NTZND model (22), the Lyapunov function candidate [4, 7] is generalized as

$$L_1(\mathbf{x}(t), t) = \frac{1}{2}\|\varepsilon(\mathbf{x}(t), t)\|_2^2 + \frac{1}{2}\gamma\left\|\int_0^t \varepsilon(\mathbf{x}(\tau), \tau)\mathrm{d}\tau\right\|_2^2, \quad \text{(A.1)}$$

where $\varepsilon(\mathbf{x}(t), t) = A(t)\mathbf{x}(t) - \mathbf{b}(t)$. It is evident that $L_1(\mathbf{x}(t), t) \geq 0$. According to NTZND model (22), we have

$$\begin{aligned} &A(t)\dot{\mathbf{x}}(t) + \dot{A}(t)\mathbf{x}(t) - \dot{\mathbf{b}}(t) \\ &\quad = -\lambda\varepsilon(\mathbf{x}(t), t) - \gamma\int_0^t \varepsilon(\mathbf{x}(\tau), \tau)\,\mathrm{d}\tau, \end{aligned} \quad \text{(A.2)}$$

which can be rewritten as

$$\dot{\varepsilon}(\mathbf{x}(t), t) = -\lambda\varepsilon(\mathbf{x}(t), t) - \gamma\int_0^t \varepsilon(\mathbf{x}(\tau), \tau)\,\mathrm{d}\tau. \quad \text{(A.3)}$$

Thus, for each element of $\varepsilon(\mathbf{x}(t), t)$, i.e., $\varepsilon_i(\mathbf{x}(t), t)$, we have

$$\dot{\varepsilon}_i(\mathbf{x}(t), t) = -\lambda\varepsilon_i(\mathbf{x}(t), t) - \gamma\int_0^t \varepsilon_i(\mathbf{x}(\tau), \tau)\,\mathrm{d}\tau. \quad \text{(A.4)}$$

Based on the above result, we have the following theoretical derivation about the time derivative of Lyapunov function candidate $L_1(\mathbf{x}(t), t)$.

$$\begin{aligned} &\dot{L}_1(\mathbf{x}(t), t) \\ &\quad = \sum_{i=1}^{m_1} \varepsilon_i(\mathbf{x}(t), t)\dot{\varepsilon}_i(\mathbf{x}(t), t) + \gamma\sum_{i=1}^{m_1}\int_0^t \varepsilon_i(\mathbf{x}(\tau), \tau)\,\mathrm{d}\tau\varepsilon_i(\mathbf{x}(t), t) \\ &\quad = \sum_{i=1}^{m_1} \varepsilon_i(\mathbf{x}(t), t)\left(-\lambda\varepsilon_i(\mathbf{x}(t), t) - \gamma\int_0^t \varepsilon_i(\mathbf{x}(\tau), \tau)\,\mathrm{d}\tau\right) \\ &\qquad + \gamma\sum_{i=1}^{m_1}\int_0^t \varepsilon_i(\mathbf{x}(\tau), \tau)\,\mathrm{d}\tau\varepsilon_i(\mathbf{x}(t), t) \\ &\quad = -\lambda\sum_{i=1}^{m_1}\varepsilon_i^2(\mathbf{x}(t), t) \\ &\quad \leq 0. \end{aligned} \quad \text{(A.5)}$$

Owing to the Lyapunov theory in research [4, 7], it further infers that $L_1(\mathbf{x}(t), t) \geq 0$ and $\dot{L}_1(\mathbf{x}(t), t) \leq 0$, which represents that the residual error of first-layer $\|A(t)\mathbf{x}(t) - \mathbf{b}(t)\|_2$ globally converges to zero as $t \longrightarrow +\infty$. Besides, based on NTZND model (22), we have $C(t)\dot{\mathbf{x}}(t) + E(t)\mathbf{x}(t) - \mathbf{d}(t) = 0$, and thus, the residual error of the second layer of HMTVLES (4), i.e., $\|C(t)\dot{\mathbf{x}}(t) + E(t)\mathbf{x}(t) - \mathbf{d}(t)\|_2$ also globally converges to zero. Finally, it is proved that when the solution of NTZND model (22) starts from any initial state $\mathbf{x}(t_0)$, residual error defined as $\|A(t)\mathbf{x}(t) - \mathbf{b}(t)\|_2 + \|C(t)\dot{\mathbf{x}}(t) + E(t)\mathbf{x}(t) - \mathbf{d}(t)\|_2$ globally converges to zero as $t \longrightarrow +\infty$.

B. Proof Process of Theorem 2

We define $\int_0^t \varepsilon(\tau)\,\mathrm{d}\tau$ as $\mathbf{y}(t)$, and thus have $\dot{\mathbf{y}}(t) = \varepsilon(t)$ and $\ddot{\mathbf{y}}(t) = \dot{\varepsilon}(t)$. Based on NTZND model (22), we have

$$\dot{\varepsilon}(t) = -\lambda\varepsilon(t) - \gamma\int_0^t \varepsilon(\tau)\,\mathrm{d}\tau, \quad \text{(B.1)}$$

which is exactly

$$\ddot{\mathbf{y}}(t) = -\lambda\dot{\mathbf{y}}(t) - \gamma\mathbf{y}(t). \quad \text{(B.2)}$$

Considering any element of $\mathbf{y}(t)$, we have

$$\ddot{y}(t) = -\lambda\dot{y}(t) - \gamma y(t). \quad \text{(B.3)}$$

Its characteristic roots can be calculated as $\alpha_1 = (-\lambda + \sqrt{\lambda^2 - 4\gamma})/2$ and $\alpha_2 = (-\lambda - \sqrt{\lambda^2 - 4\gamma})/2$. The analytical solution to (27) can be divided into the following three cases.

(1) If $\lambda^2 - 4\gamma = 0$, the roots α_1 and α_2 are equally real numbers, i.e., α, and then we have

$$y(t) = \varepsilon_i(0)t\,\exp(\alpha t). \quad \text{(B.4)}$$

Thus,

$$\varepsilon_i(t) = \dot{y}(t) = \varepsilon_i(0)\exp(\alpha t) + \varepsilon_i(0)\alpha t\ \exp(\alpha t). \tag{B.5}$$

(2) If $\lambda^2 - 4\gamma > 0$, the roots α_1 and α_2 are different real numbers, and we have

$$y(t) = \frac{\varepsilon_i(0)\left(\exp(\alpha_1 t) - \exp(\alpha_2 t)\right)}{\sqrt{\lambda^2 - 4\gamma}}. \tag{B.6}$$

Then,

$$\varepsilon_i(t) = \dot{y}(t) = \frac{\varepsilon_i(0)\left(\alpha_1 \exp(\alpha_1 t)\right) - \alpha_2 \exp(\alpha_2 t)}{\sqrt{\lambda^2 - 4\gamma}}. \tag{B.7}$$

(3) If $\lambda^2 - 4\gamma < 0$, the roots α_1 and α_2 are conjugate complex numbers, i.e., $\alpha_1 = a + ib$ and $\alpha_2 = a - ib$. Then, we have

$$y(t) = \frac{\varepsilon_i(0)\sin(bt)\exp(\mathrm{at})}{b}. \tag{B.8}$$

Then,

$$\varepsilon_i(t) = \dot{y}(t) = \varepsilon_i(0)\exp(\mathrm{at})\left(\frac{a\ \sin(bt)}{b} + \cos(bt)\right). \tag{B.9}$$

Summarizing the previous analysis of the three situations and according to the proof of Theorem 1, we have the conclusion that, starting from any initial condition, the residual error of first-layer $\|\varepsilon(t)\|_2$ exponentially converges to zero as $t \longrightarrow +\infty$. Besides, based on NTZND model (22), we have $C(t)\dot{\mathbf{x}}(t) + E(t)\mathbf{x}(t) - \mathbf{d}(t) = 0$, and thus, the residual error of the second layer of HMTVLES (4), i.e., $\|C(t)\dot{\mathbf{x}}(t) + E(t)\mathbf{x}(t) - \mathbf{d}(t)\|_2$ also exponentially converges to zero. Finally, it is proved that residual error of NTZND model (22) for solving HMTVLES (4) exponentially converges to zero as $t \longrightarrow +\infty$.

C. Proof Process of Theorem 3

According to the Laplace transformation [4–6], the NTZND model (23) leads to

$$s\varepsilon_i(s) - \varepsilon_i(0) = -\lambda\varepsilon_i(s) - \frac{\gamma}{s}\varepsilon_i(s) + \eta_i(s), \tag{C.1}$$

where $\eta_i(s)$ represents the Laplace transformation of $\eta_i(t)$. Computing the above equation yields

$$\varepsilon_i(s) = \frac{s(\varepsilon_i(0) + \eta_i(s))}{s^2 + s\lambda + \gamma}. \tag{C.2}$$

The corresponding transfer function is $s/(s^2 + s\lambda + \gamma)$. The poles of the transfer function are $s_1 = (-\lambda + \sqrt{\lambda^2 - 4\gamma})/2$ and $s_2 = 0(-\lambda - \sqrt{\lambda^2 - 4\gamma})/2$. The poles of transfer function are located on the left half plane, which means that model (23) is stable. Since the noise is constant, we have $\eta_i(s) = \eta_i/s$. Using the final value theorem, we have

$$\begin{aligned}
&\lim_{t\to\infty}\varepsilon_i(t),\\
&= \lim_{s\to 0} s\varepsilon_i(s),\\
&= \lim_{s\to 0}\frac{s^2(\varepsilon_i(0) + \eta_i/s)}{s^2 + s\lambda + \gamma} = 0.
\end{aligned} \tag{C.3}$$

Besides, based on NTZND model (22), the equation $C(t)\dot{\mathbf{x}}(t) + E(t)\mathbf{x}(t) - \mathbf{d}(t) = 0$ is satisfied. Finally, it is proved that residual error of model (23) for solving HMTVLES (4) converges to zero as $t \longrightarrow +\infty$.

D. Proof Process of Theorem 4

According to the Laplace transformation [4–6], the NTZND model (23) leads to

$$s\varepsilon_i(s) - \varepsilon_i(0) = -\lambda\varepsilon_i(s) - \frac{\gamma}{s}\varepsilon_i(s) + \eta/s^2. \tag{D.1}$$

Computing the above equation yields

$$\varepsilon_i(s) = \frac{s\left(\varepsilon_i(0) + \eta/s^2\right)}{s^2 + s\lambda + \gamma}. \tag{D.2}$$

Using the final value theorem, we have

$$\begin{aligned}
&\lim_{t\to\infty}\varepsilon_i(t)\\
&= \lim_{s\to 0} s\varepsilon_i(s)\\
&= \lim_{s\to 0}\frac{s^2\left(\varepsilon_i(0) + \eta/s^2\right)}{s^2 + s\lambda + \gamma} = \frac{\eta}{\gamma}.
\end{aligned} \tag{D.3}$$

Besides, based on NTZND model (22), the equation $C(t)\dot{\mathbf{x}}(t) + E(t)\mathbf{x}(t) - \mathbf{d}(t) = 0$ is satisfied. Finally, it is proved that residual error of model (23) for solving HMTVLES (4) converges to η/γ as $t \longrightarrow +\infty$.

E. Proof Process of Theorem 5

NTZND model (23) leads to

$$\dot{\varepsilon}_i(t) = -\lambda\varepsilon_i(t) - \gamma\int_0^t \varepsilon_i(\tau)\,\mathrm{d}\tau + \eta_i(t), \tag{E.1}$$

where $\eta_i(t)$ denotes any element of the bounded unknown vector-form random noise. According to the values of λ and γ, the analyses can be divided into the following three situations:

(1) For $\lambda^2 > 4\gamma$, the solution to subsystem (28) can be obtained as

$$\begin{aligned}\varepsilon_i(t) = {} & \frac{\varepsilon_i(0)\left(\alpha_1\exp\left(\alpha_1 t\right) - \alpha_2\exp\left(\alpha_2 t\right)\right)}{\left(\alpha_1-\alpha_2\right)} \\ & + \left(\int_0^t \left(\alpha_1\exp\left(\alpha_1\left(t-\tau\right)\right)\right) - \alpha_2\exp\left(\left(\alpha_2\left(t-\tau\right)\right)\right)\right. \\ & \left. \cdot\, \eta_i(\tau)\,\mathrm{d}\tau\right)\frac{1}{\left(\alpha_1-\alpha_2\right)}.\end{aligned} \tag{E.2}$$

From the triangle inequality, we have

$$\begin{aligned}\left|\varepsilon_i(t)\right| \le {} & \frac{\left|\varepsilon_i(0)\left(\alpha_1\exp\left(\alpha_1 t\right) - \alpha_2\exp\left(\alpha_2 t\right)\right)\right|}{\left(\alpha_1-\alpha_2\right)} \\ & + \frac{\int_0^t \left\|\alpha_1\exp\left(\alpha_1\left(t-\tau\right)\right)\right\|\eta_i(\tau)|\mathrm{d}\tau|}{\left(\alpha_1-\alpha_2\right)} \\ & + \frac{\int_0^t\left|\alpha_2\exp\left(\alpha_2\left(t-\tau\right)\right)\right|\left\|\eta_i(\tau)|\mathrm{d}\tau\right|}{\left(\alpha_1-\alpha_2\right)}.\end{aligned} \tag{E.3}$$

We further have

$$\begin{aligned}\left|\varepsilon_i(t)\right| \le {} & \frac{\left|\varepsilon_i(0)\left(\alpha_1\exp\left(\alpha_1 t\right) - \alpha_2\exp\left(\alpha_2 t\right)\right)\right|}{\left(\alpha_1-\alpha_2\right)} \\ & + \frac{2}{\left(\alpha_1-\alpha_2\right)}\max\nolimits_{0\le\tau\le t}\left|\eta_i(\tau)\right| \\ = {} & \frac{\left|\varepsilon_i(0)\left(\alpha_1\exp\left(\alpha_1 t\right) - \alpha_2\exp\left(\alpha_2 t\right)\right)\right|}{\left(\alpha_1-\alpha_2\right)} \\ & + \frac{2}{\sqrt{\lambda^2-4\gamma}}\max\nolimits_{0\le\tau\le t}\left|\eta_i(\tau)\right|.\end{aligned} \tag{E.4}$$

Finally, we have

$$\lim_{t\longrightarrow\infty}\sup\left\|\varepsilon(t)\right\|_2 \le \frac{2m_1}{\sqrt{\lambda^2-4\gamma}}\sup\nolimits_{0\le\tau\le t}\left|\eta_i(\tau)\right|. \tag{E.5}$$

(2) For $\lambda^2 = 4\gamma$, the solution to subsystem (28) can be obtained as

$$\begin{aligned}\varepsilon_i(t) = {} & \varepsilon_i(0)t\alpha_1\exp\left(\alpha_1 t\right) + \varepsilon_i(0)\exp\left(\alpha_1 t\right) \\ & + \int_0^t\left(\left(t-\tau\right)\alpha_1\exp\left(\alpha_1\left(t-\tau\right)\right)\right)\eta_i(\tau)\mathrm{d}\tau \\ & + \int_0^t\exp\left(\alpha_1\left(t-\tau\right)\right)\eta_i(\tau)\mathrm{d}\tau,\end{aligned} \tag{E.6}$$

where $\theta_1 = (-\lambda + \sqrt{\lambda^2-4\gamma})/2, = -\gamma/2..$ We know that there exist $\mu > 0$ and $\nu > 0$, such that

$$\left|\alpha_1\right|t\exp\left(\alpha_1 t\right) \le \mu\exp\left(-\nu t\right). \tag{E.7}$$

Thus, based on the above inequality as well as the triangle inequality, we have

$$\begin{aligned}\left|\varepsilon_i(t)\right| \le {} & \left|\varepsilon_i(0)\left(\alpha_1 t\exp\left(\alpha_1 t\right) + \exp\left(\alpha_1 t\right)\right)\right| \\ & + \int_0^t\mu\exp\left(-\nu\left(t-\tau\right)\right)\eta_i(\tau)|\mathrm{d}\tau| \\ & + \int_0^t\left|\exp\left(\alpha_1\left(t-\tau\right)\right)\right\|\eta_i(\tau)\left|\right|\mathrm{d}\tau|.\end{aligned} \tag{E.8}$$

We further have

$$\begin{aligned}\varepsilon_i(t)| \le {} & \left|\varepsilon_i(0)\left(\alpha_1 t\exp\left(\alpha_1 t\right) + \exp\left(\alpha_1 t\right)\right)\right. \\ & + \left(\frac{\mu}{\nu} - \frac{1}{\alpha_1}\right)\max\nolimits_{0\le\tau\le t}\left|\eta_i(\tau)\right|.\end{aligned} \tag{E.9}$$

Finally, we have

$$\lim_{t\longrightarrow\infty}\sup\left\|\varepsilon(t)\right\|_2 \le \left(\frac{\mu}{\nu} - \frac{1}{\alpha_1}\right)m_1\sup\nolimits_{0\le\tau\le t}\left|\eta_i(\tau)\right|. \tag{E.10}$$

(3) For $\lambda^2 < 4\gamma$, the solution to subsystem (28) can be obtained as

$$\begin{aligned}\varepsilon_i(t) = {} & \varepsilon_i(0)\exp(\alpha t)\left(\frac{\alpha\sin\left(\beta t\right)}{\beta} + \cos\left(\beta t\right)\right) + \\ & \int_0^t\left(\begin{array}{c}\dfrac{\alpha\sin\left(\beta\left(t-\tau\right)\right)\exp\left(\alpha\left(t-\tau\right)\right)}{\beta} \\ \\ +\cos\left(\beta\left(t-\tau\right)\right)\exp\left(\alpha\left(t-\tau\right)\right)\end{array}\right)\eta_i(\tau)\,\mathrm{d}\tau,\end{aligned} \tag{E.11}$$

where $\alpha = -\gamma/2$ and $\beta = \sqrt{4\gamma-\lambda^2})/2$. Thus, based on triangle inequality, we can similarly have

$$\begin{aligned}|\varepsilon_i(t)| &\leq \left|\varepsilon_i(0)\exp(\alpha t)\left(\frac{\alpha\sin(\beta t)}{\beta+\cos(\beta t)}\right)\right| \\ &\quad - \frac{\sqrt{\alpha^2+\beta^2}}{\alpha\beta}\max_{0\leq\tau\leq t}|\eta_i(\tau)| \\ &= \left|\varepsilon_i(0)\exp(\alpha t)\left(\frac{\alpha\sin(\beta t)}{\beta+\cos(\beta t)}\right)\right| \\ &\quad + \frac{4\gamma}{\lambda\sqrt{4\gamma-\lambda^2}}\max_{0\leq\tau\leq t}|\eta_i(\tau)|.\end{aligned} \tag{E.12}$$

Finally, we have

$$\lim_{t\longrightarrow\infty}\sup\|\varepsilon(t)\|_2 \leq \frac{4\gamma m_1}{\lambda\sqrt{4\gamma-\lambda^2}}\sup_{0\leq\tau\leq t}|\eta_i(\tau)|. \tag{E.13}$$

Residual error of NTZND model (22) for solving HMTVLES (4) in the presence of unknown vector-form random noise $\eta(t)\in\mathbb{R}^{m_1}$, i.e., model (23), is approximately in inverse proportion to λ as $t\longrightarrow+\infty$.

The above analysis of the three situations show that, in the presence of the bounded unknown vector-form random noise, residual error of NTZND model (23) is bounded by $2m_1\sup_{0\leq\tau\leq t}|\eta_i(\tau)|/\sqrt{\lambda^2-4\gamma}$ for $\lambda^2>4\gamma$, or $4m_1\gamma\sup_{0\leq\tau\leq t}|\eta_i(\tau)|/(\lambda\sqrt{4\gamma-\lambda^2})$ for $\lambda^2<4\gamma$. That is, the upper bound of $\lim_{t\longrightarrow\infty}\|\varepsilon(t)\|_2$ is approximately in inverse proportion to λ.

F. Proof Process of Theorem 6

Similar to the proof of Theorem 1, the Lyapunov function candidate is generalized as

$$L_1(\mathbf{x}(t),t) = \frac{1}{2}\|\varepsilon(\mathbf{x}(t),t)\|_2^2 + \frac{1}{2}\gamma\left\|\int_0^t\varepsilon(\mathbf{x}(\tau),\tau)\,\mathrm{d}\tau\right\|_2^2, \tag{F.1}$$

where $\varepsilon(\mathbf{x}(t),t) = A(t)\mathbf{x}(t)-\mathbf{b}(t)$. It is evident that $L_1(\mathbf{x}(t),t)\geq 0$. For each element of $\varepsilon(t)$, i.e., $\varepsilon_i(t)$, we have

$$\dot{\varepsilon}_i(\mathbf{x}(t),t) = -\lambda\varphi(\varepsilon_i(\mathbf{x}(t),t)) - \gamma\int_0^t\varepsilon_i(\mathbf{x}(\tau),\tau)\,\mathrm{d}\tau. \tag{F.2}$$

Based on the above result, we have the following theoretical derivation about the time derivative of Lyapunov function candidate $L_1(\mathbf{x}(t),t)$.

$$\begin{aligned}\dot{L}_1(\mathbf{x}(t),t) &= \sum_{i=1}^{m_1}\varepsilon_i(\mathbf{x}(t),t)\dot{\varepsilon}_i(\mathbf{x}(t),t) + \gamma\sum_{i=1}^{m_1}\int_0^t\varepsilon_i(\mathbf{x}(\tau),\tau)\,\mathrm{d}\tau\,\mathrm{d}\tau\varepsilon_i(\mathbf{x}(t),t) \\ &= \sum_{i=1}^{m_1}\varepsilon_i(\mathbf{x}(t),t)\left(-\lambda\varphi(\varepsilon_i(\mathbf{x}(t),t)) - \gamma\int_0^t\varepsilon_i(\mathbf{x}(\tau),\tau)\,\mathrm{d}\tau\right) \\ &\quad + \gamma\sum_{i=1}^{m_1}\int_0^t\varepsilon_i(\mathbf{x}(\tau),\tau)\,\mathrm{d}\tau\varepsilon_i(\mathbf{x}(t),t) \\ &= -\lambda\sum_{i=1}^{m_1}\varepsilon_i(\mathbf{x}(t),t)\varphi(\varepsilon_i(\mathbf{x}(t),t)).\end{aligned} \tag{F.3}$$

As assumed that $\varphi(\cdot)$ is monotonically-increasing odd activation function, we have

$$\varphi(\varepsilon_i(\mathbf{x}(t),t))\begin{cases}>0, & \text{when } \varepsilon_i(\mathbf{x}(t),t)>0,\\ =0, & \text{when } \varepsilon_i(\mathbf{x}(t),t)=0,\\ <0, & \text{when } \varepsilon_i(\mathbf{x}(t),t)<0.\end{cases} \tag{F.4}$$

Thus, we have

$$-\lambda\sum_{i=1}^{m_1}\varepsilon_i(\mathbf{x}(t),t)\varphi(\varepsilon_i(\mathbf{x}(t),t))\leq 0. \tag{F.5}$$

Owing to the Lyapunov theory in research [4, 7], it further infers that $L_1(\mathbf{x}(t),t)\geq 0$ and $\dot{L}_1(\mathbf{x}(t),t)\leq 0$, which represents that the residual error of first-layer $\|A(t)\mathbf{x}(t)-\mathbf{b}(t)\|_2$ globally converges to zero as $t\longrightarrow+\infty$. Besides, based on general NTZND model (26), we have $C(t)\dot{\mathbf{x}}(t)+E(t)\mathbf{x}(t)-\mathbf{d}(t)=0$, and thus, the residual error of the second layer of HMTVLES (4), i.e., $\|C(t)\dot{\mathbf{x}}(t)+E(t)\mathbf{x}(t)-\mathbf{d}(t)\|_2$ also globally converges to zero. Finally, it is proved that when the solution of general NTZND model (26) starts from any initial state $\mathbf{x}(t_0)$, residual error globally converges to zero as $t\longrightarrow+\infty$.

Data Availability

Codes can be found here at https://github.com/lijcit/1511895678.

Conflicts of Interest

The authors declare that they have no conflicts of interest.

Acknowledgments

This work was supported by the National Natural Science Foundation of China (nos. 62006205, 62002307, and 61906164), by the China Postdoctoral Science Foundation funded project (with number 2021TQ0299), by the Henan Province Science and Technology Planning Project (nos. 212102310993, 212102210392), by Natural Science Foundation of Henan Province (no. 222300420274), by the Natural Science Foundation of Jiangsu Province of China (no. BK20190875), and by Nanhu Scholars Program for Young Scholars of XYNU.

References

[1] A. Simonetto and E. Dall'Anese, "Prediction-correction algorithms for time-varying constrained optimization," *IEEE Transactions on Signal Processing*, vol. 65, no. 20, pp. 5481–5494, Oct. 2017.

[2] A. Simonetto, A. Koppel, A. Mokhtari, G. Leus, and A. Ribeiro, "Decentralized prediction-correction methods for networked time-varying convex optimization," *IEEE Transactions on Automatic Control*, vol. 62, no. 11, pp. 5724–5738, Nov. 2017.

[3] L. Jin, Y. Zhang, and B. Qiu, "Neural network-based discrete-time Z-type model of high accuracy in noisy environments for solving dynamic system of linear equations," *Neural Computing & Applications*, vol. 29, no. 11, pp. 1217–1232, 2018.

[4] L. Jin, Y. Zhang, S. Li, and Y. Zhang, "Noise-tolerant ZNN models for solving time-varying zero-finding problems: a control-theoretic approach," *IEEE Transactions on Automatic Control*, vol. 62, no. 2, pp. 992–997, 2017.

[5] L. Jin, Y. Zhang, and S. Li, "Integration-enhanced Zhang neural network for real-time-varying matrix inversion in the presence of various kinds of noises," *IEEE Transactions on Neural Networks and Learning Systems*, vol. 27, no. 12, pp. 2615–2627, 2016.

[6] L. Jin, Y. Zhang, S. Li, and Y. Zhang, "Modified ZNN for time-varying quadratic programming with inherent tolerance to noises and its application to kinematic redundancy resolution of robot manipulators," *IEEE Transactions on Industrial Electronics*, vol. 63, no. 11, pp. 6978–6988, 2016.

[7] Z. Sun, F. Li, L. Jin, T. Shi, and K. Liu, "Noise-tolerant neural algorithm for online solving time-varying full-rank matrix Moore-Penrose inverse problems: a control-theoretic approach," *Neurocomputing*, vol. 413, pp. 158–172, 2020.

[8] H. G. Kocken, M. Ahlatcioglu, and I. Albayrak, "Finding the fuzzy solutions of a general fully fuzzy linear equation system," *Journal of Intelligent and Fuzzy Systems*, vol. 30, no. 2, pp. 921–933, 2016.

[9] F. Barbieri and O. L. V. Costa, "A mean-field formulation for the mean-variance control of discrete-time linear systems with multiplicative noises," *International Journal of Systems Science*, vol. 51, no. 10, pp. 1825–1846, 2020.

[10] D. Chen, Y. Zhang, S. Li, and Y. Lin, "Robust Zhang neural network for tracking control of parallel robot manipulators with unknown parameters," in *Proceedings of the 31st Chinese Control and Decision Conference*, pp. 3527–3532, IEEE, Nanchang, China, June2019.

[11] L. Jin, S. Li, B. Hu, M. Liu, and J. Yu, "A noise-suppressing neural algorithm for solving the time-varying system of linear equations: a control-based approach," *IEEE Transactions on Industrial Informatics*, vol. 15, no. 1, pp. 236–246, Jan. 2019.

[12] H.-H. Chen, M. T. Manry, and H. Chandrasekaran, "A neural network training algorithm utilizing multiple sets of linear equations," *Neurocomputing*, vol. 25, no. 1-3, pp. 55–72, 1999.

[13] K. N. B. Murthy and C. S. R. Murthy, "A new Gaussian elimination-based algorithm for parallel solution of linear equations," *Computers & Mathematics with Applications*, vol. 29, no. 7, pp. 39–54, 1995.

[14] D. S. Parker, "Schur complements obey Lambek's categorial grammar: a," *Linear Algebra and Its Applications*, vol. 278, no. 1-3, pp. 63–84, 1998.

[15] D. Jakoveti, N. Kreji, N. K. Jerinki, G. Malaspina, and A. Micheletti, "Distributed fixed point method for solving systems of linear algebraic equations," *Automatica*, vol. 134, Article ID 109924, 2021.

[16] M. Mimura and N. Tokushige, "Solving linear equations in a vector space over a finite field," *Discrete Math*, vol. 344, no. 12, Article ID 112603, 2021.

[17] Y. Zhang, Y. Ling, S. Li, M. Yang, and N. Tan, "Discrete-time zeroing neural network for solving time-varying Sylvester-transpose matrix inequation via exp-aided conversion," *Neurocomputing*, vol. 386, pp. 126–135, 2020.

[18] Y. Zhang, L. He, C. Hu, J. Guo, J. Li, and Y. Shi, "General four-step discrete-time zeroing and derivative dynamics applied to time-varying nonlinear optimization," *Journal of Computational and Applied Mathematics*, vol. 347, pp. 314–329, 2019.

[19] Y. Zhang, L. Ming, H. Huang, J. Chen, and Z. Li, "Time-varying Schur decomposition via Zhang neural dynamics," *Neurocomputing*, vol. 419, pp. 251–258, 2021.

[20] J. Li, Y. Zhang, and M. Mao, "General square-pattern discretization formulas via second-order derivative elimination for zeroing neural network illustrated by future optimization," *IEEE Transactions on Neural Networks and Learning Systems*, vol. 30, no. 3, pp. 891–901, 2019.

[21] J. Li, Y. Zhang, and M. Mao, "Five-instant type discrete-time ZND solving discrete time-varying linear system, division and quadratic programming," *Neurocomputing*, vol. 331, pp. 323–335, 2019.

[22] J. Li, M. Mao, F. Uhlig, and Y. Zhang, "A 5-instant finite difference formula to find discrete time-varying generalized matrix inverses, matrix inverses, and scalar reciprocals," *Numerical Algorithms*, vol. 81, no. 2, pp. 609–629, 2019.

[23] Y. Zhang, S. Li, and G. Geng, "Initialization-based k-winners-take-all neural network model using modified gradient descent," *IEEE Transactions on Neural Networks and Learning Systems*, pp. 1–9, 2021.

[24] L. Xiao, S. Li, K. Li, L. Jin, and B. Liao, "Co-design of finite-time convergence and noise suppression: a unified neural model for time varying linear equations with robotic applications," *IEEE Transactions on Systems, Man, and Cybernetics: Systems*, vol. 50, no. 12, pp. 5233–5243, 2020.

[25] Z. Zhang, L. Zheng, T. Qiu, and F. Deng, "Varying-parameter convergent-differential neural solution to time-varying overdetermined system of linear equations," *IEEE Transactions on Automatic Control*, vol. 65, no. 2, pp. 874–881, 2020.

[26] Z. Zhang, L. Zheng, and T. Qiu, "A gain-adjustment neural network based time-varying underdetermined linear equation solving method," *Neurocomputing*, vol. 458, pp. 184–194, 2021.

[27] B. Qiu, Y. Zhang, and Z. Yang, "New discrete-time ZNN models for least-squares solution of dynamic linear equation system with time-varying rank-deficient coefficient," *IEEE Transactions on Neural Networks and Learning Systems*, vol. 29, no. 11, pp. 5767–5776, 2018.

[28] L. Xiao, Y. He, B. Liao, and J. Dai, "An accelerated ZNN-based algorithm with piecewise time-varying parameters to solve time-variant linear equations," *Journal of Computational and Applied Mathematics*, vol. 398, p. 113665, 2021.

[29] L. Jia, L. Xiao, J. Dai, Z. Qi, Z. Zhang, and Y. Zhang, "Design and application of an adaptive fuzzy control strategy to

zeroing neural network for solving time-variant QP problem," *IEEE Transactions on Fuzzy Systems*, vol. 29, no. 6, pp. 1544–1555, 2021.

[30] L. Xiao, Y. Zhang, J. Dai, Q. Zuo, and S. Wang, "Comprehensive analysis of a new varying parameter zeroing neural network for time varying matrix inversion," *IEEE Transactions on Industrial Informatics*, vol. 17, no. 3, pp. 1604–1613, 2021.

[31] L. Xiao, Y. Cao, J. Dai, L. Jia, and H. Tan, "Finite-time and predefined-time convergence design for zeroing neural network: theorem, method, and verification," *IEEE Transactions on Industrial Informatics*, vol. 17, no. 7, pp. 4724–4732, 2021.

[32] L. Xiao, J. Dai, L. Jin, W. Li, S. Li, and J. Hou, "A Noise-enduring and finite-time zeroing neural network for equality-constrained time-varying nonlinear optimization," *IEEE Transactions on Systems, Man, and Cybernetics: Systems*, vol. 51, no. 8, pp. 4729–4740, 2021.

[33] L. Xiao, Y. Zhang, Q. Zuo, J. Dai, J. Li, and W. Tang, "A noise-tolerant zeroing neural network for time-dependent complex matrix inversion under various kinds of noises," *IEEE Transactions on Industrial Informatics*, vol. 16, no. 6, pp. 3757–3766, 2020.

[34] Y. Shi, W. Zhao, S. Li, B. Li, and X. Sun, "Novel discrete-time recurrent neural network for robot manipulator: a direct discretization technical route," *IEEE Transactions on Neural Networks and Learning Systems*, pp. 1–10, 2021.

[35] Y. Shi, L. Jin, S. Li, J. Li, J. Qiang, and D. K. Gerontitis, "Novel discrete-time recurrent neural networks handling discrete-form time-variant multi-augmented Sylvester matrix problems and manipulator application," *IEEE Transactions on Neural Networks and Learning Systems*, vol. 33, no. 2, pp. 587–599, 2022.

[36] J. Li, Y. Zhang, and M. Mao, "Continuous and discrete zeroing neural network for different-level dynamic linear system with robot manipulator control," *IEEE Transactions on Systems, Man, and Cybernetics: Systems*, vol. 50, no. 11, pp. 4633–4642, 2020.

[37] F. Xu, Z. Li, Z. Nie, H. Shao, and D. Guo, "Zeroing neural network for solving time-varying linear equation and inequality systems," *IEEE Transactions on Neural Networks and Learning Systems*, vol. 30, no. 8, pp. 2346–2357, 2019.

[38] W. Wu and B. Zheng, "Two new Zhang neural networks for solving time-varying linear equations and inequalities systems," *IEEE Transactions on Neural Networks and Learning Systems*, pp. 1–9, 2021.

[39] M. Yang, Y. Zhang, H. Hu, and B. Qiu, "General 7-Instant DCZNN model solving future different-level system of nonlinear inequality and linear equation," *IEEE Transactions on Neural Networks and Learning Systems*, vol. 31, no. 9, pp. 3204–3214, 2020.

[40] J. Guo, B. Qiu, J. Chen, and Y. Zhang, "Solving future different-layer nonlinear and linear equation system using new eight-node DZNN model," *IEEE Transactions on Industrial Informatics*, vol. 16, no. 4, pp. 2280–2289, 2020.

[41] B. Qiu, J. Guo, X. Li, and Y. Zhang, "New discretized zeroing neural network models for solving future system of bounded inequalities and nonlinear equations aided with general explicit linear four-step rule," *IEEE Transactions on Industrial Informatics*, vol. 17, no. 8, pp. 5164–5174, 2021.

[42] M. Yang, Y. Zhang, N. Tan, M. Mao, and H. Hu, "7-instant discrete-time synthesis model solving future different-level linear matrix system via equivalency of zeroing neural network," *IEEE Transactions on Cybernetics*, pp. 1–10, 2021.

[43] J. Guo, B. Qiu, and Y. Zhang, "Future different-layer linear equation and bounded inequality solved by combining Adams-Bashforth methods with CZNN model," *IEEE Transactions on Industrial Electronics*, vol. 68, no. 2, pp. 1515–1524, 2021.

[44] J. Li, X. Zhu, Y. Shi, J. Wang, and H. Guo, "Real-time robot manipulator tracking control as multilayered time-varying problem," *Applied Mathematical Modelling*, vol. 96, pp. 355–366, 2021.

[45] J. Li, M. Mao, Y. Zhang, and B. Qiu, "Different-level algorithms for control of robotic systems," *Applied Mathematical Modelling*, vol. 77, pp. 922–933, 2020.

[46] J. Li, R. Yao, Y. Feng, S. Wang, and X. Zhu, "Zeroing neural network for solving hybrid multilayered time-varying linear system," *IEEE Access*, vol. 8, pp. 199406–199414, 2020.

[47] L. Jin, L. Wei, and S. Li, "Gradient-based differential neural-solution to time-dependent nonlinear optimization," *IEEE Transactions on Automatic Control*1 page, 2022.

[48] M. Liu, L. Chen, X. Du, L. Jin, and M. Shang, "Activated gradients for deep neural networks," *IEEE Transactions on Neural Networks and Learning Systems*, pp. 1–13, 2021.